Broadband Cognitive Radio Enabled by Photonics

Dan Zhu, *Member, IEEE*, and Shilong Pan, *Senior Member, IEEE*

(Invited Paper)

***Abstract*—Cognitive radio is considered as a possible disruptive force to improve the spectral resource efficiency through sensing and interacting with the environment. Traditional electrical technologies to implement the cognitive radio face challenges in terms of bandwidth, resolution, and speed. In this paper, the concept and architecture of broadband cognitive radio systems enabled by photonics are proposed. Key microwave photonic techniques for the architecture are reviewed, including the photonics-based spectrum sensing, the photonic arbitrary waveform generation, the photonics-based self-interference cancellation processing, and the microwave photonic dechirp processing and radar imaging. A preliminary demonstration of a cognitive radar system enabled by photonics is performed. The future possible research directions on this topic are discussed.**

***Index Terms*—Cognitive radio, microwave photonics, spectrum sensing, waveform generation, self-interference cancellation, radar imaging.**

I. Introduction

A GLOBAL challenge faced by modern wireless systems is to develop new services covering broad bandwidth with limited available spectrum source. Conventional radio-frequency (RF) systems work independently and have no interaction with the environment. Thus, it usually has to allocate a static frequency spectrum to exclusive licensed users. With the wireless devices and systems increasing explosively, the electromagnetic environment becomes more and more complex, and the available spectrum is increasingly scarce.

Cognitive radio technology is considered to be a possible disruptive force within the spectrum management, making the RF system work effectively, reliably and robustly in a complex electromagnetic environment [1], [2]. Unlike traditional RF systems, cognitive RF systems learn, infer and react to the environment, which can be described as OODA (i.e., observe, orient, decide, act) loops, as illustrated in Fig. 1 [2], [3]. The environment is first observed through different kinds of sensors. The information is then processed by a cognitive processor and oriented to infer the meanings based on prior knowledge. A decision is made and sent to a dynamic control system, which configures the transceiver to act according to the environmental changes. In this way, the cognitive radio system can dynamically allocate the RF spectrum resources for RF applications.

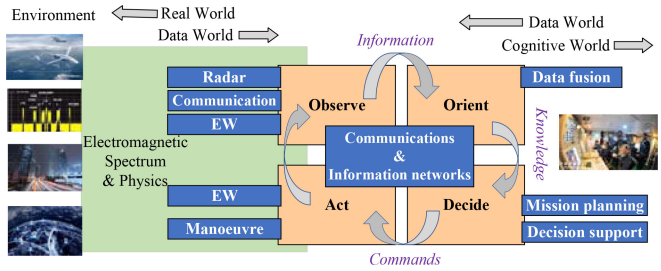

Fig. 1. Cognitive RF system described as an OODA loop. OODA: observe, orient, decide, and act [3].

A conceptual scheme of the cognitive radio system has been proposed in [1], which is mainly composed of the cognitive radio platform and the cognitive controlling part. The cognitive radio platform realizes the functions of spectrum sensing, and adaptive signal generation and processing over a wide frequency range. Meanwhile, the cognitive controlling part orients the meaning of the observed information, makes decisions, and controls the cognitive radio platform.

Typical approaches for implementing the cognitive radio platform primarily comprise analog RF front-ends, analog-to-digital converts (ADCs), digital signal processors (DSPs), and digital-to-analog converters (DACs). The key difference between these platforms is originated from the architecture of the analog RF front-ends after antennas and RF amplification chains. One such architecture applies a number of switches, frequency converters and narrow-band filters to cover a wide bandwidth, while others employ tunable RF components to improve the flexibility of bandwidth and operation frequency. Complex platform configurations have to be applied if the system needs to have broad bandwidth due to the factor that the ADCs to sample the input RF signals usually have a limited effective number of bits at high frequency, the DSPs to extract the information from the input signals would encounter intolerable latency and power consumption if the amount of data is huge, and the DACs to produce the waveforms can output signals in the low-frequency regime with relatively small bandwidth. In addition, the cognitive radio system generally exploits multiple RF functions to observe the environment, such as radar imaging and electromagnetic spectrum sensing. The devices, layer structure, and optimal frequency bands for different RF functions are diverse. Challenges in interoperability, including the coexistence, cooperation, and

Manuscript received November 15, 2019; revised March 19, 2020; accepted May 3, 2020. Date of publication May 7, 2020; date of current version June 16, 2020. This work was supported in part by the National Natural Science Foundation of China under Grant 61971222, in part by the Jiangsu Provincial Program for High-level Talents in Six Areas under Grant DZXX-030, and in part by the Fundamental Research Funds for Central Universities under Grants NE2017002 and NC2018005. *(Corresponding author: Shilong Pan.)*

The authors are with the Key Laboratory of Radar Imaging and Microwave Photonics Ministry of Education Nanjing University of Aeronautics and Astronautics, Nanjing 210016, China (e-mail: danzhu@nuaa.edu.cn; pans@ieee.org).

Color versions of one or more of the figures in this article are available online at http://ieeexplore.ieee.org.

Digital Object Identifier 10.1109/JLT.2020.2993021

TABLE I
PERFORMANCE COMPARISON BETWEEN MICROWAVE TECHNIQUES AND MICROWAVE PHOTONIC TECHNIQUES FOR COGNITIVE RADIO

	Microwave System	Microwave Photonic Technique
Frequency Range	Tens of GHz	THz
Instantaneous Bandwidth	Several GHz	Tens of GHz
Transmission Loss	~0.6 dB/m	0.0002 dB/m
EMI	Serious	Immune
SWaP	High	Low
Isolation	Low	High

EMI: electromagnetic interference; SWaP: size, weight, and power consumption.

collaboration of different function layers exist, and the increase of the size, weight and power consumption (SWaP) is inevitable.

Microwave photonics is considered to be an effective solution to these problems [4]–[7], due to the advantages of wideband and real-time signal generation, transmission, controlling and processing capability brought by photonics. Table I lists several key advantages for establishing the cognitive radio system by introducing microwave photonics, as compared with those using traditional microwave techniques. As can be seen, the innovative implementation of the cognitive radio system will be allowed with significant added values based on microwave photonics.

Recently, we have proposed the concept and architecture of the broadband cognitive radio enabled by photonics [5]. In this paper, the key microwave photonic techniques to establish the cognitive radio system are reviewed, including photonics-based spectrum sensing, photonic arbitrary waveform generation, and photonic signal processing. Recent experimental studies to establish the cognitive radio system based on microwave photonics are introduced. The future possible research directions are also discussed.

II. THE ARCHITECTURE OF THE PHOTONICS-BASED COGNITIVE RADIO

The basic concept of the cognitive radio enabled by photonics is illustrated in Fig. 2. The system is mainly composed of the inputs and outputs (IOs), the photonic cognitive radio platform and the radio artificial intelligence (AI) cognitive processing module. The IOs contains the wideband RF amplification chains. The photonic cognitive radio platform consists of three main parts: (1) the photonic spectrum sensor to realize the real-time spectrum sensing of the ultra-wideband electromagnetic environment; (2) the photonic signal generator to produce wideband adaptive waveform; (3) the photonic signal processor to realize the real-time processing of the wideband signals.

The photonic spectrum sensor realizes the real-time spectrum sensing of the ultra-wideband electromagnetic environment. The complex electromagnetic environment brings great challenges to realize the spectrum sensing using traditional electrical technologies. Microwave photonic spectrum sensing approaches

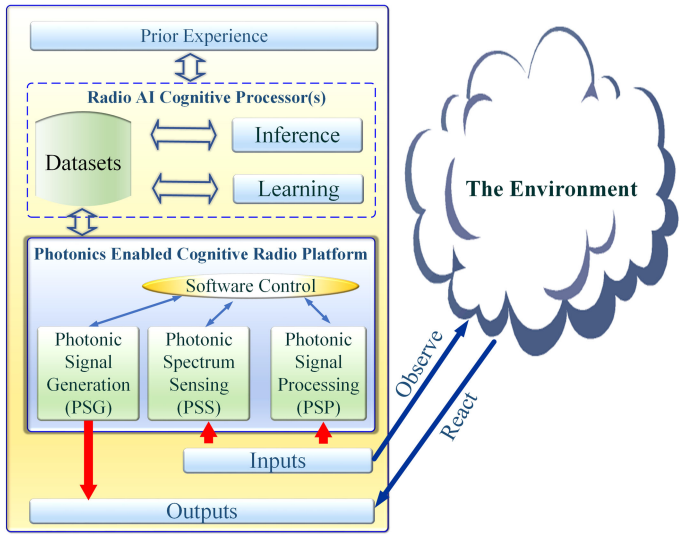

Fig. 2. The concept of the cognitive radio enabled by photonics.

have the advantages of wide instantaneous bandwidth, immunity to electromagnetic interference and parallel fast sensing ability.

The photonic signal generator realizes the function of generating RF waveforms. Since the generated RF signals should be flexibly adjusted according to the complex electromagnetic environment, the signal generator must be reconfigurable over a wide bandwidth. Photonic approaches have been demonstrated to have the capability of broadband arbitrary waveform generation with high performance.

The photonic signal processor realizes the processing of the received RF signals. If the received RF signals cover a wide bandwidth, the response speed of the cognitive radio system needs to be fast. In addition, for the cognitive radio system, the capabilities of in-band full-duplex operation and spectral efficiency improvement over a wide frequency range are needed, leading to the requirement of the self-interference cancellation over a large bandwidth. Thanks to the advantages of wide bandwidth, parallel signal processing and low transmission loss introduced by photonics, high processing speed over a wide operation bandwidth will be enabled.

The operation process of the system is as follows. The photonic spectrum sensor observes the ultra-wideband electromagnetic environment. The observed information is fed back to the radio AI cognitive processors to orient the meaning. A decision will be made accordingly and applied to control the photonic signal generator to generate the optimal RF signals. The photonic signal processor is also adjusted to process the received signals and achieve the required functions decided by the cognitive system. In this way, a broadband cognitive radio system can be established to address various challenges of the pure electronic implementation, thanks to the advantages introduced by photonics. For instance, the photonic cognitive radio demonstrated in [5] easily achieved an instantaneous bandwidth of 4 GHz in the frequency range of 17.5-26 GHz, while the bandwidth of the electronic approaches is around tens of MHz [8].

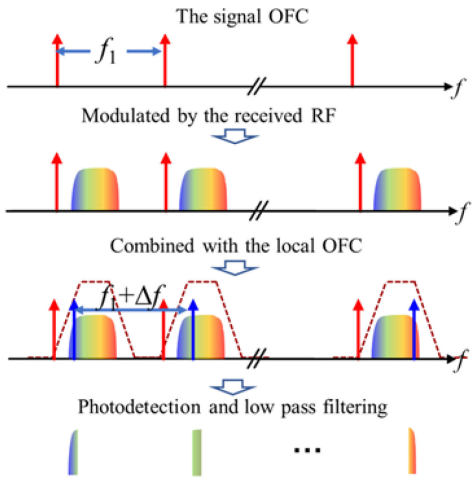

Fig. 3. Coherent optical channelization based on two OFCs.

TABLE II
PERFORMANCE COMPARISON OF COHERENT CHANNELIZERS BASED ON OFCS

Ref.	RF BW (GHz)	CBW (GHz)	CN	IRR (dB)	OFC Comb-line number
[26]	11.89-12.21	0.08	4	None	5
[28]	DC-19	1.04	20	None	20
[31]	3.75-7.25	0.5	7	>35 (single tone)	7
[32]	24-30	0.5	12	N/A	12
[34]	Over 30	6	5	>30 (over 10 MHz BW)	5
[35]	13-18	1	5	>25 (over 1 GHz BW)	5
[36]	7-13	1	6	>25 (over 1 GHz BW)	3
[37]	Over 30	1.2	8	>20 (over 1.2 GHz BW)	1

BW: bandwidth; CBW: channel bandwidth; CN: channel number; IRR: image rejection ratio.

III. KEY TECHNOLOGIES FOR THE PHOTONICS-BASED COGNITIVE RADIO

Previously, various microwave photonic techniques that might be applied to the architecture in Fig. 2 were demonstrated, including the photonics-based spectrum sensing, the photonic arbitrary waveform generation, the photonics-based self-interference cancellation processing, and the microwave photonic dechirp processing and radar imaging. This section provides a brief review of these techniques and discusses the benefits that might be brought by them.

A. Photonics-Based Spectrum Sensing

Microwave photonic spectrum sensing approaches have been widely studied in recent years [9], [10]. Typical methods include optical channelization [11]–[37], photonics-based frequency scanning [39]–[49], and optical Fourier transform [50]–[58].

The basic function of channelization is to slice the received spectrum into a number of narrowband parallel channels, which can then be processed by low-speed electronics [59]. One straightforward way to implement the microwave channelization in the optical domain is based on an array of optical filters [11]–[23], but the crosstalk, channel bandwidth and channel consistency are usually restricted by the limited performance of the optical filters. To solve this problem, coherent optical channelization was proposed [24]–[28]. One typical scheme is based on parallel photonic mixing and two OFCs with slightly different spacing [26]–[29], as shown in Fig. 3. The RF signal is broadcasted to each comb line of the signal OFC, and the local OFC serves as a photonic LO bank to downconvert different RF components from different optically carried copies. Since these RF components have been well separated in the optical domain by using the OFC, optical filters with low requirements are sufficient to split them into a series of different channels.

Thanks to the square-law detection nature of photodetectors, the components of the signal located at the left and right sides of the comb line in the local OFC would be downconverted simultaneously and overlapped in the frequency domain [30]. One approach to solve this problem is to introduce in-phase/quadrature (I/Q) demodulation and electrical digital signal processing [31]–[33] or to apply microwave photonic image-reject mixers (IRMs) [30], [34]–[37]. Another issue associated with the coherent optical channelization is that a large number of high-quality comb lines are required to achieve broadband spectrum sensing with high resolution. Previously, we proposed a microwave photonic dual-output IRM based on balanced Hartley architecture, which can reduce the requirement of the comb line number by half [36], [38]. By further applying the polarization multiplexing technique [37], the requirement of the comb line number can be reduced to 1/8. The performance of different coherent optical channelizers based on dual OFCs is summarized in Table II.

Photonics-based frequency scanning is another effective method for spectrum sensing, which follows the concept of frequency scanning receiver in the electrical domain and can be realized by sweeping the frequency of a photonic LO [39]–[42], an optically carried RF signal [43]–[46], or the response of an optical filter [47]–[49]. Table III compares the performances of the spectrum sensing based on different methods in this category.

Fourier transform is a widely-used and mature method for spectrum sensing, especially in the digital domain [50]. With the increase of the bandwidth, the amount of data to be processed will be huge. The relatively-low processing speed of the DSPs would hinder real-time operation, and the power dissipation is considerable. Many approaches have been proposed to realize the Fourier transform in the optical domain [51]–[58], by which the spectrum information of the input RF signal is directly mapped into the time domain and obtained without using DSPs.

One intuitive method to realize the optical Fourier transform is based on an optical dispersive medium [51]–[54]. The concept comes from the space-time duality, referring to the similarity between the diffraction of an electromagnetic beam in the space domain and dispersive propagation of an electromagnetic pulse

TABLE III
PERFORMANCE COMPARISON OF SPECTRUM SENSING METHODS BASED ON PHOTONICS-BASED FREQUENCY SCANNING

Ref.	RF BW [GHz]	Scanning Channel number	Channel Spacing (GHz)	Scanning time/channel (s)	Frequency Resolution (Hz)
[39]	0-18	6	3	0.2μ/0.4μ	5M/2.5M
[40]	0-20	10	2	0.5μ	2M
[41]	14	7	2	0.4μ	2.5 M
[42]	0.5-28.5	28	1	10m	<100k
[43] [46]	0.1-20	80	0.25	1.5μ	250M
[44]	0-40	4	12	0.05μ	20 M
[45]	0-12	6	2	0.4μ	2.5 M
[47]	2-30	N/A	N/A	N/A	375M
[48]	0.5-28	N/A	N/A	N/A	20M
[49]	12-18	N/A	N/A	N/A	100M

BW: bandwidth.

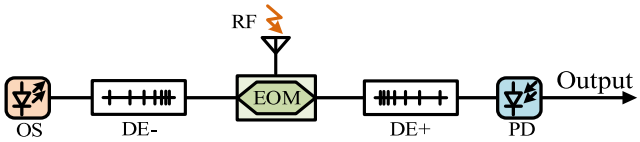

Fig. 4. Real-time Fourier transform system based on time-frequency convolution. OS: optical source, EOM: electro-optical modulator, DE: dispersion element, PD: photodetector.

in the time domain [51]. Fraunhofer diffraction in the space domain realizes the Fourier transform of the input beam. Similarly, in the time domain, when a short optical pulse passes through a dispersion medium, the pulse spectrum will be mapped into the time domain. By modulating the electrical signal to be measured to the optical pulse, the Fourier transform of the optically carried signal will be accomplished [52]–[53]. To improve the frequency resolution, the method of bandwidth magnification is proposed and demonstrated [54].

Fourier transform can also be implemented by using a photonics-based temporal convolution system [55], as shown in Fig. 4. An ultra-short optical pulse passes through a temporal stretching medium, an electro-optical modulator (EOM) and a temporal compression medium, and then injected into a photodetector (PD). The temporal stretching medium and the temporal compression medium are realized by two dispersive mediums with inverse dispersion values. The spectrum of the applied RF signal is mapped into the time domain at the output of the system. To reduce the requirement of the ADC sampling rate for the output waveform observation, the technologies of temporal amplification [56] and asynchronous optical sampling [57] are utilized. Recently, an optical frequency-shifted loop is established to implement the Fourier transform [58]. The RF signal to be measured is first converted into the optical domain, which is then shifted in the optical frequency-shifted loop both in the time domain and in the frequency domain. The mathematical expression of the optical output of the loop is adjusted to match with the Fourier transform definition. Table IV compares the performances of the photonics-based Fourier transform systems.

TABLE IV
PERFORMANCE COMPARISON OF PHOTONICS-BASED FOURIER TRANSFORM SYSTEMS

Ref.	Instantaneous Bandwidth (Hz)	Frequency Resolution (Hz)	Frame rate (Hz)
[53]	200 G	N/A	N/A
[54]	2.52 G	25 M	50 M
[55]	21 G	1.5 G	N/A
[56]	20 G	1 G	50 M
[57]	28 G	100 M	1 k
[58]	12.89 M	30 k	77 M

For the broadband cognitive radio applications, the three kinds of spectrum sensing approaches have their respective advantages and disadvantages. The optical channelization approaches are reliable and effective, but there is a tradeoff between the bandwidth and the resolution, and a large amount of hardware resources might be consumed due to the parallel structure. For the photonics-based frequency scanning approaches, the required hardware resources are effectively reduced, but the cost is the relatively-large response time. The photonics-based Fourier transform can realize a fast measurement over a large bandwidth, but the dynamic range needs improvement for practical applications. For the cognitive radio system, the selection of the spectrum sensing method depends on the requirement of the application. For example, photonics-based frequency scanning may be applied if the interference in the environment is slowly varied, while the photonics-based Fourier transform can be deployed in the scenario when the interference is strong.

B. Photonic Arbitrary Waveform Generation

Photonic arbitrary waveform generation can be achieved based on optical spectral shaping and frequency-to-time mapping [60]–[68], time-domain synthesis [69]–[84], and photonic DAC [85]–[98].

Optical spectral shaping and frequency-to-time mapping for arbitrary waveform generation are usually implemented based on ultrashort optical pulses [60]–[68]. The frequency components of the optical pulses are firstly shaped via an optical spectral shaping device, and then go through a dispersive device to map the spectral profile into the time domain. After optical to electrical conversion, a microwave arbitrary waveform can be obtained. One key component in the system is the optical spectral shaping module, which should be reconfigurable to adapt to the cognitive radio applications. Previously, the optical spectral shaping module was realized by programmable spatial light modulators [60], [62], fiber Bragg gratings (FBGs) [65], and ring resonator-based optical filters [66].

Time-domain synthesis can also be exploited to generate flexible microwave waveforms. One typical example is realized based on the injection of semiconductor lasers [69]–[84]. The optically injected semiconductor laser is operated in the period-one (P1) oscillation state. An optical carrier and a sideband with its frequency dependent on the injection strength and wavelength are generated at the output of the laser. After optical to electrical conversion, a microwave waveform will be

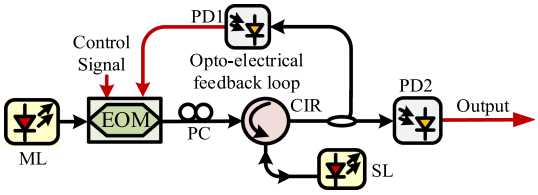

Fig. 5. Microwave waveform generation based on an optically injected semiconductor laser with a control signal to configure the generated microwave signal and an optoelectronic feedback loop to improve the signal quality.

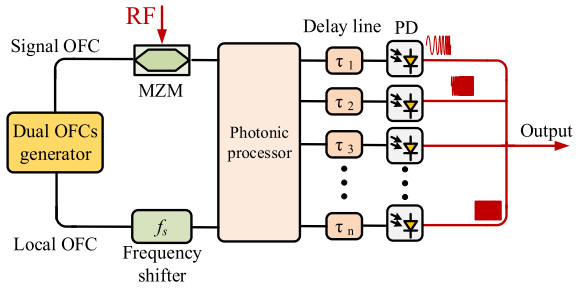

Fig. 6. Photonic microwave waveform generation based on OFCs. MZM: Mach-Zehnder modulator.

generated. By controlling the optical injection strength and/or the frequency detuning between the master laser and the slave laser, microwave waveform with tunable frequency will be generated. Previously, reconfigurable microwave waveforms including the CW/pulsed, linearly chirped and frequency-hopping signals were successfully generated [79]–[83]. The quality of the generated microwave waveform can be improved by injecting a low-frequency stable subharmonic microwave signal [73] or introducing all-optical or optoelectronic feedback loops [74]–[77]. Fig. 5 shows an example for reconfigurable waveform generation with improved quality based on this kind of method, which applies an external control signal and a feedback signal simultaneously to an EOM inserted between the master laser and the slave laser [84].

Similar to electronic DACs, photonic DAC is another effective way to generate arbitrary waveforms [85]–[98]. In general, the photonic DAC can be implemented using a parallel or serial architecture. In the parallel structure [85]–[94], the lightwave is divided into N channels. The nth channel is set to have a weighted optical power of 2^n times the power in the first channel. Then, these channels are modulated by a number of digital inputs and summed in the PD. Since the parallel photonic DAC converts multiple bits at the same time, the speed is high. But the effectiveness of the system is limited by the extinction ratio of the EOMs. In the serial photonic DAC, a serial bit stream is used as the input, and the digital-to-analog conversion is implemented by optical gating of the delayed and weighted signals [95] or by pulse pattern recognition [96]. Since the modulation and summation can be implemented in a single channel, the system is simplified. But a strict requirement of time delay control is needed.

Among different kinds of waveforms, linear frequency modulated (LFM) microwave waveforms are widely applied in a variety of RF applications thanks to the capability of pulse compression [99]. Various microwave photonic approaches to generate the LFM waveform has been proposed [100]–[126]. One intuitive method is the optical heterodyne between a pre-chirped optical pulse and a CW lightwave [100], a fast wavelength-sweeping laser and a CW laser [101]–[102], or two time-delayed quadratically frequency-modulated optical pulses [103]. The methods, however, face challenges of poor linearity, small time-bandwidth product, or limited bandwidth. These problems can be easily solved by the waveform synthesis methods based on OFCs [104]–[105]. Taking the scheme in [105] as an example, two coherent OFCs with a slightly different comb line spacing are used, as shown in Fig. 6. An IF-LFM signal is used to modulate the signal OFC. The modulated signal OFC is combined with the local OFC, and spliced into different channels. If signals in these channels are sent to optical to electrical converters, LFM signals with different center frequencies will be generated. If a series of time delays are introduced to the channels and combining them in the optical domain, LFM signals with both the time duration and bandwidth multiplied can be generated. The time-bandwidth product of the generated LFM signal can be improved by $N \times N$ times, and the linearity is improved by N times, where N is the used comb line number. The LFM waveforms can also be generated based on the Fourier domain mode-locked optoelectronic oscillators (OEOs) [106]–[110]. Besides, investigations are also taken in the microwave photonic dual-chirp LFM signal generation [111]–[122] to avoid the range-Doppler coupling effect of the single-chirp LFM signal [123]–[125].

Different photonics-based waveform generation approaches would be best suitable for the generation of one or two specific waveform types, and have their own merits and shortcomings. For the broadband cognitive radio systems, the selection of the photonics-based waveform generation method depends on the aimed function of the system. Meanwhile, the compatibility of the system with the other functional blocks of the cognitive radio system should be taken into consideration.

C. *Photonics-Based Self-Interference Cancellation Processing*

Photonics-based self-interference cancellation [127]–[132] can be used to achieve wideband and high isolation between the transmitter and the receiver of a cognitive radio system. The basic idea of self-interference cancellation is to introduce a small portion of the transmitted signal as the reference signal to the receiver. The received RF signal (containing the interference) and the reference signal are modulated to the optical domain, respectively. The optically carried reference signal is properly delayed, power weighted, phase inverted, and then combined with the optically carried RF signal, by which the interference in the received signal is canceled. Wideband phase inversion is the key to implement the optical self-interference cancellation, which can be realized in the optical domain by using counter-biasing modulations [128], the out-of-phase property of the phase-modulated sidebands [129], a microwave photonic

TABLE V
PERFORMANCE COMPARISON OF PHOTONIC SELF-INTERFERENCE CANCELLATION APPROACHES

	single tone / narrow-band		broad-band	
Ref.	RF band	c depth [dB]	RF band	c depth [dB]
[128]	@ 3 GHz	73	96 MHz @ 3 GHz	33
[129]	@ 5 GHz @ 8 GHz	57 56	10 MHz@ 5 GHz 10MHz @ 8 GHz	20 19
[130]	N/A	N/A	13.3 GHz @ 10 GHz 9.5 GHz @ 10 GHz	20 30
[131]	10 kHz @ 900 MHz and 2.4 GHz	65	50 MHz @ 900 MHz 40 MHz @ 2.4 GHz	40 30
[132]	N/A	N/A	500MHz @ 4.9 GHz	37.2
[133]	N/A	N/A	50 MHz @ 2.4 GHz 200 MHz @2.4 GHz	30 40
[134]	N/A	N/A	50 MHz @ 3 GHz	30
[136, 137]	N/A	N/A	1 GHz @ 10 GHz 1 GHz @ 16 GHz	18 18

c depth: cancellation depth.

phase shifter [130], balanced photodetection [131] or an RF balun [132].

Multipath interference due to the reflection, diffraction and scattering is another issue that must be considered in a realistic scenario. This can be addressed by establishing an optical compensation branch with a parallel set of weighted time-delay lines. In [133], the optical compensation branch is realized by inserting a number of parallel fiber delay lines and optical power attenuators; while in [134], an array of tunable lasers are used, and the delays and the magnitudes are tuned by adjusting the wavelength and the optical power of each laser.

Since the interference signals reflected from different materials may have frequency-independent phase shifts, they would not be canceled with only a fixed π-phase shift. To remedy this, microwave photonic phase shifters based on a polarization modulator is applied to introduce tunable phase shifts [130]. In addition, it would be interesting that the self-interference cancellation is implemented together with frequency mixing from the practical point of view. Recently, approaches to simultaneously realize the self-interference cancellation and image-reject mixing are demonstrated based on a DP-QPSK modulator [135], or a polarization multiplexed 90° optical hybrid [136]–[137].

According to [138], a typical narrow-band cancellation depth for Wi-Fi and cellular applications is 110 dB, and the active analog cancellation should contribute 30-45 dB. The performance of typical photonic self-interference cancellation approaches in the literature is summarized in Table V. As can be seen, the photonics-based self-interference cancellation can provide more than 56-dB cancellation depth for narrowband applications. Some implementation can provide a cancellation depth of more than 30 dB over a 9.5-GHz bandwidth [130], which is not possible for the state-of-the-art electronic approaches.

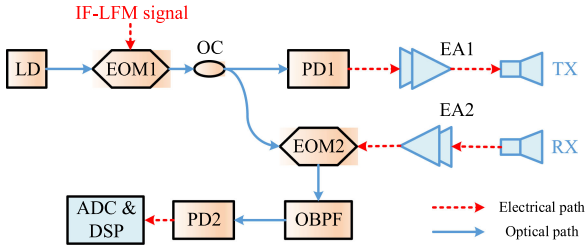

Fig. 7. Photonic dechirp processing combined with microwave photonic signal generation.

D. Microwave Photonic Dechirp Processing and Radar Imaging

Since imaging radar has the capability of working under all day and all weather conditions, it is one of the most important sensors for a cognitive radio system to observe the physical environment. Synthetic aperture radar imaging (SAR) and Inverse synthetic aperture radar (ISAR) imaging are two popular techniques for radar imaging. They both use the relative movement between the radar and target to create a synthetic aperture, which provides fine spatial resolution. The range resolution of the imaging radar is mainly determined by the bandwidth of the transmitted signal. Consequently, to meet the requirements for ultra-high resolution observation, a large instantaneous bandwidth is needed. In addition, fast signal processing is essential to realize real-time imaging.

Imaging radar based on microwave photonics can generate and process signals with large bandwidth, which is highly required by a cognitive radio system. Many photonics-based radar systems have been reported. The first photonics-based fully digital radar called “PHODIR” was reported in 2014 [6]. A mode-locked laser (MLL) is used to generate reconfigurable waveforms for the transmitter and provide ultra-low jitter sampling pulse for the photonic analog to digital conversion in the receiver, respectively. Later, several microwave photonic imaging radar systems utilizing photonic dechirp processing and/or microwave photonic signal generation have been proposed [139]–[147]. To implement the dechirp processing, the radar waveform is typically an LFM signal. The received echo is mixed with the reference signal, generating an IF signal. The sensing information, including the time delay and the Doppler frequency and so on, will be effectively converted into the output IF signal, which usually has a narrow bandwidth and a low frequency.

The typical way to achieve the photonics-based dechirp processing is to perform the mixing in the optical domain [139]. The bandwidth and frequency can be further extended by combing the microwave photonic signal generation [140]–[143]. As shown in Fig. 7, the optical carrier is modulated by an IF-LFM signal at EOM1. The obtained optical signal is divided into two parts. One part is sent into PD1 to perform the optical-to-electrical conversion. By properly adjusting the bias voltage of EOM1, frequency doubling [140], quadrupling [141]–[142] or sextupling [143] will be achieved. An RF signal with the instantaneous bandwidth multiplied is generated. The other part

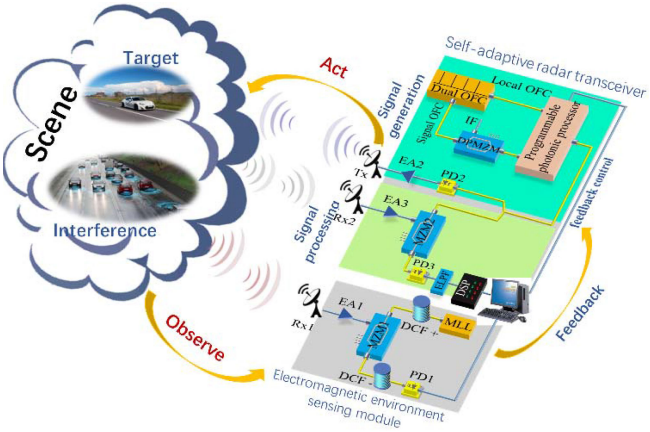

Fig. 8. Schematic of the photonics-based broadband cognitive radar. EA: electrical amplifier; ELPF: electrical low-pass filter; DSP: digital signal processing; MLL: mode-locked laser; DCF: dispersion compensating fiber.

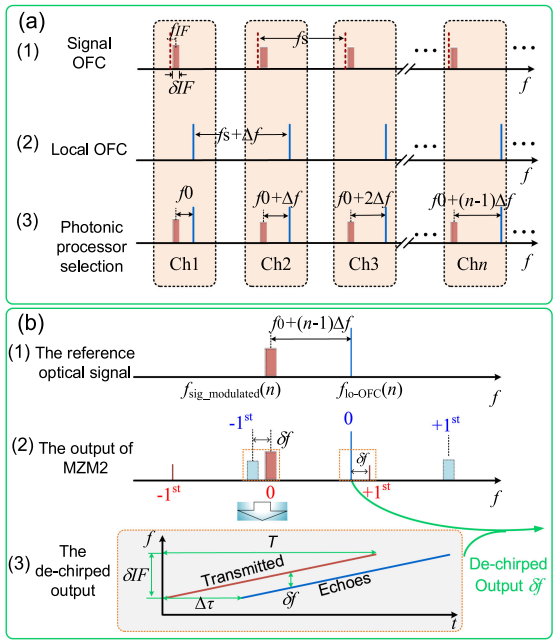

Fig. 9. The principle of the signal generation and processing in the microwave photonic transceiver. (a) The radar waveform generation and (b) the signal dechirping.

of the optical signal is injected into EOM2, which is driven by the received RF echo. By injecting the output optical signal into PD2, the dechirp processing is successfully achieved. Furthermore, in [144], a balanced I/Q dechirp receiver is established by introducing the photonic IRM based on the balanced Hartley structure [38]. Both the image interference and the undesired mixing spurs are suppressed simultaneously for the dechirp processing in the optical domain.

It should be noted that the microwave photonic dechirp processing can also be used for multi-band radars [145]–[150]. The key challenge is to process different band signals simultaneously, and make the sensing information from different bands not interfere with each other. In [145], the polarization multiplexing and de-multiplexing are introduced to realize the dechirp processing of dual-band LFM signals. Another way is to introduce a specially designed integrated dual-band LFM waveform with inverse chirp rates [146]–[147], which can be received simultaneously and detected independently. To distinguish the de-chirped outputs of different bands, a third auxiliary chirp signal is added in [146], while the photonic I/Q mixing is introduced in [147]. With the multi-band operation capability enabled by photonics, multiple RF functions can be implemented in a single system, such as radar and communication [151] and radar imaging and frequency measurement [152].

IV. Demonstration of Microwave Photonic Cognitive System

Based on the proposed photonic cognitive radio architecture, and the key enabling microwave photonic technologies, a demo of a cognitive radar system enabled by photonics is performed. Fig. 8 shows the schematic diagram of the proposed photonics-based broadband cognitive radar, which is mainly composed of two parts, i. e., a real-time electromagnetic environment sensing module and a microwave photonic self-adaptive radar transceiver. Real-time sensing of the environment is first achieved by using photonics-based real-time Fourier transform (RTFT). The obtained environment information is used to adjust the microwave photonic transceiver, by which frequency-agility RF signal generation based on dual OFCs and photonic dechirp processing for radar imaging are implemented. A low-frequency narrowband signal is then produced and real-time ISAR imaging with high resolution is realized.

The RTFT for electromagnetic environment sensing is built based on temporal convolution. Firstly, an ultra-short optical pulse with a wideband spectrum is generated by an MLL. After passing through a dispersive element with a dispersion value of Φ_0, the pulse is time-stretched and the profile of the stretched pulse is consistent with its spectrum, realizing spectrum-to-time mapping. The electrical signals received from the environment are lead to MZM1 to modulate the stretched optical pulse. The modulated optical signal is propagated through a second dispersive element with a dispersion value of $-\Phi_0$, by which the pulse is recompressed. The frequency of the received electrical signal is therefore transformed into the time domain, and the RTFT process is realized with a frequency-to-time coefficient of Φ_0. By simply analyzing the output temporal waveform, the frequency spectra of the received RF signals from the electromagnetic environment can be obtained.

The microwave photonic radar transceiver can self-adaptively select the proper frequency band for target detection according to the observed environment information. Fig. 9 illustrates the principle of the microwave photonic radar transceiver, which is constructed based on two OFCs. A signal OFC and a local OFC with the free spectral ranges (FSRs) of f_S and $f_S+\Delta f$, respectively, are used. For the radar waveform generation, the signal OFC is modulated by an IF signal centered at f_{IF} with a bandwidth of δ_{IF} and a time duration of T based on the carrier suppressed single sideband (CS-SSB) modulation, as shown in

Fig. 9(a1). A programmable photonic processor is used to select the optically-carried IF signal and the corresponding photonic LO comb line, as shown in Fig. 9(a3). The selected optical signal is then divided into two parts. One part is injected into PD2 to generate the radar waveform. By selecting the required optical components through the programmable photonic processor, the center frequency of the radar waveforms can be tuned according to the environment information. The generated signal is amplified by EA2 and radiated to the free space through an antenna for target detection.

The other part of the optical signal from the programmable photonic processor is served as the reference signal to realize the dechirp processing of the radar echoes in the optical domain, with the principle shown in Fig. 9(b). The echoes from the targets are collected by an antenna, amplified by EA3, and used to modulate the reference optical signal at MZM2. As can be seen in Fig. 9(b1), the reference signal in the nth channel contains two optical components of $f_{\text{lo-OFC}}(n)$ and $f_{\text{sig\_modulated}}(n)$. After modulation at MZM2, a few new components are generated, with the optical spectrum illustrated in Fig. 9(b2). By leading the optical output of MZM2 into PD3, a low-frequency de-chirped signal will be produced. It should be noted that the obtained de-chirped signal comes from two parts, as shown in Fig. 9(b3). One part is the beating signal between the optical component of $f_{\text{sig\_modulated}}(n)$ and the -1st-order signal sideband generated from the optical carrier of $f_{\text{lo-OFC}}(n)$. The other part is the beating signal between the optical component of $f_{\text{lo-OFC}}(n)$ and the $+1$st signal sideband generated from the optical carrier of $f_{\text{sig\_modulated}}(n)$. Based on the dechirp processing output, ISAR imaging can be realized through the two-dimensional Fourier transform.

In an experiment, a microwave photonic cognitive radar with two-band (17.5–21.5 GHz and 22–26 GHz) frequency agility is established. Self-adaptive anti-jamming ISAR imaging is achieved in the presence of interference. In the photonics-based self-adaptive radar transceiver, a signal OFC and a local OFC with 3 comb lines are used. The FSRs of the two OFCs are 31 and 35.5 GHz, respectively, and the frequency spacing between the 1st comb lines of the two OFCs is adjusted to be 30 GHz. An IF-LFM signal centered at 6 GHz with a bandwidth of 4 GHz and a time duration of 30 μs is used to modulate the signal OFC with CS-SSB modulation. The optical spectra of the signal OFC before and after modulation are shown in Fig. 10(a). The modulated signal OFC and the local OFC with the spectra shown in Fig. 10(b) are sent into the programmable photonic processor.

First, the programmable optical processor selects the 2nd channel, and an LFM signal covering 17.5–21.5 GHz is generated. The observed electrical spectrum, waveform and the instantaneous frequency-time diagram of the generated signal are shown in Figs. 11(a)–(c), respectively. To show the target detection capability of the proposed cognitive radar in the presence of interference, the imaging performance is investigated. The target is a fan with three blades placed on a turntable, as shown in Fig. 12(a). Each blade has a length of 16 cm and a width of 7.5 cm, placed about 4 cm away from the center of the turntable. The turntable is rotating in the horizontal plane with an angular speed of 360° per second. Fig. 12(b) shows the imaging

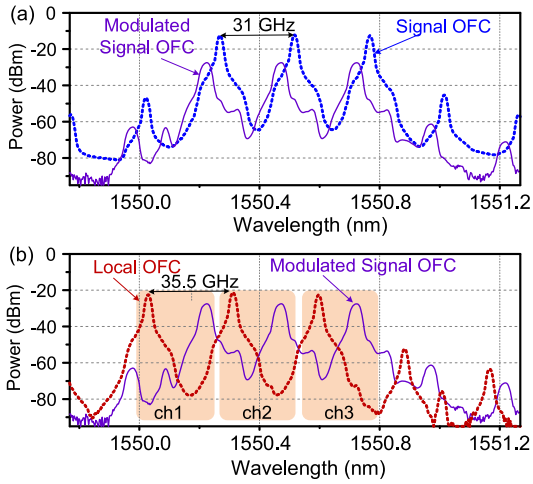

Fig. 10. Experimentally measured optical spectra of (a) the signal OFC before (dotted line) and after (solid line) modulation, (b) the local OFC (dotted line) and the modulated signal OFC (solid line) sent into the programmable photonic processor.

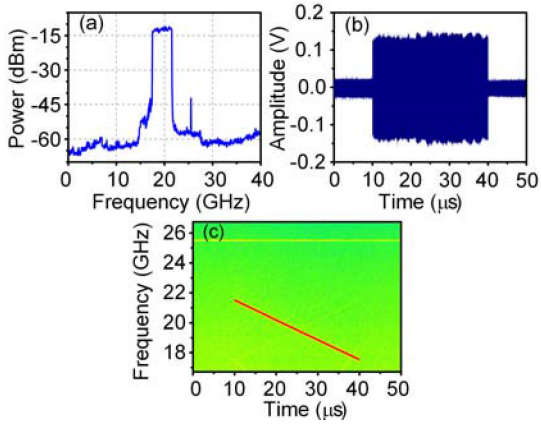

Fig. 11. (a) The measured electrical spectrum, (b) waveform, and (c) the instantaneous frequency-time diagram of the generated RF-LFM signal covering 17.5–21.5 GHz.

result. The three blades can be clearly observed. It should be mentioned that the obtained de-chirped signal is only sampled with a sampling rate of 10 MSa/s in the experiment, making real-time ISAR imaging possible.

Then the interference signal is switched to 17.5–21.5 GHz. The radar is interfered, with the imaging result shown in Fig. 13(a). The real-time spectral sensing result is shown in Fig. 13(b). The time delay between the reference pulse and the signal pulse is 100 ps and the FWHM (full width at half-maxima) of the signal pulse is 35 ps, indicating the existence of an interference signal centered at 19 GHz with a bandwidth of $\sim$6.63 GHz. According to the feedback information about the environment, the programmable optical processor is reconfigured to select the 1st channel shown in Fig. 10(b) to generate an RF-LFM signal covering 22–26 GHz. The electrical spectrum, waveform and instantaneous frequency-time diagram of the generated signal

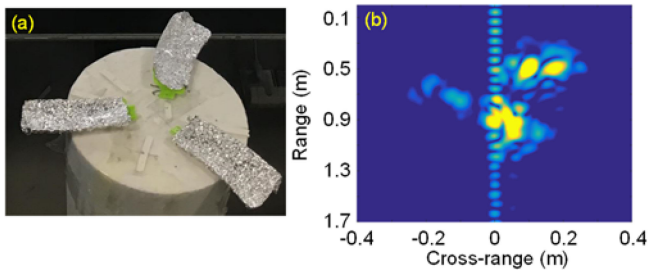

Fig. 12. (a) The target on a turntable, and (b) the imaging result when the radar is operated at 17.5–21.5 GHz.

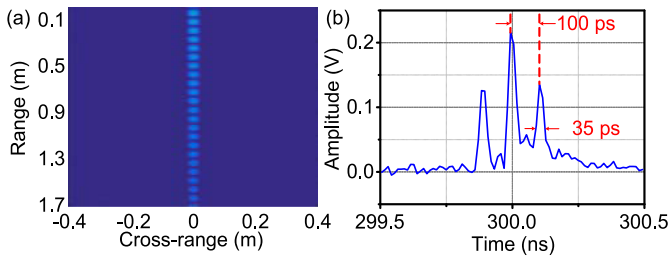

Fig. 13. (a) The imaging result and (b) the RTFT result when there is an interference signal within 17.5–21.5 GHz.

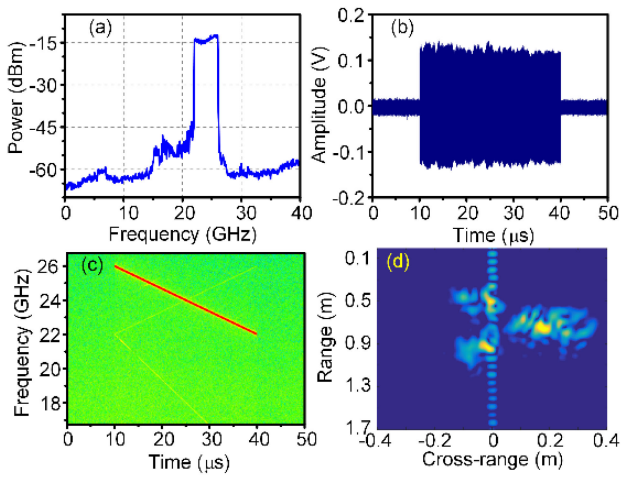

Fig. 14. (a) The measured electrical spectrum, (b) waveform and (c) the instantaneous frequency-time diagram of the generated RF-LFM signal at 22–26 GHz, and (d) the imaging result.

are shown in Figs. 14(a)–(c), respectively. ISAR imaging is successfully implemented again, with the result shown in Fig. 14(d). Therefore, the cognitive radar successfully achieves a reliable working state via interaction with the environment.

For the spectrum sensing module, by introducing a photonic dispersion medium that has short physics length, the spectrum sensing time over large bandwidth will be very short. Taking a dispersive FBG with a 1-m length as an example, the response time is calculated to be about 10 ns. The switching time of the microwave photonic transceiver is mainly determined by the programmable optical processor used to select the required optical components. In our experiment, a waveshaper is used as the programmable optical processor, whose typical response time is several ms. Recently, the integrated programmable optical processors with fast responses have been proposed [153]. By introducing these devices, the response time of the system can be further reduced.

V. Discussion and Conclusion

This article reviewed the recent advancement in microwave photonics to establish broadband cognitive radio systems. By introducing microwave photonic components and subsystems to realize real-time broadband spectrum sensing of the complex electromagnetic environment, wideband adaptive waveform generation, fast processing of the wideband signals, broadband and flexible cognitive radio system can be established.

Although the concept of microwave photonic cognitive radio was demonstrated, there is considerable room for improvement. First, the compatibility of different microwave photonic components and subsystems to establish the cognitive radio system should be improved to integrate multiple microwave photonic modules in a single platform. The spectrum sensing, waveform generation and dechirp processing modules are implemented using different laser sources, modulators and photodetectors. Second, the electromagnetic environment sensing only relies on spectrum analysis, which is insufficient. In the future, modulation format, signal strength, angle of arrival and so on should be identified for building more efficient systems. Third, the research on the cognitive radio covers multidisciplinary areas, ranging from system architecture, testbed, signal processing, control algorithms, security to network. This paper mainly deals with the challenge of broadband cognitive radio systems associated with the RF section. Other interesting issues associated with the broadband cognitive radio enabled by photonics should be taken into account. In addition, to exert the full potential of microwave photonics for the cognitive radio, the RF components involved in the system, including the antennas, the power amplifiers and dividers and so on are also required to have wide bandwidth operation capability.

Currently, integrated microwave photonics are developing rapidly [154]–[156]. More compact and reliable photonics-based spectrum sensing module and photonics-based transceiver with higher performance are expected. With the research efforts on these directions devoted to microwave photonics, the cognitive radio platform enabled by photonics is becoming an attractive and feasible approach for future radio systems such as radar, electronic warfare, wireless communication systems, and the comprehensive multi-function integration RF systems.

Acknowledgment

The authors would like to thank several individuals from the Key Laboratory of Radar Imaging and Microwave Photonics, Ministry of Education, Nanjing University of Aeronautics and Astronautics, Nanjing, China, for their assistance: Wenjuan Chen, Xiaopen Hu, Bowen Zhang, Bingdong Gao, Yue Yang, Jiewen Ding, and Jiang Liu.

REFERENCES

[1] V. T. Nguyen, F. Villain, and Y. L. Guillou, "Cognitive radio RF: Overview and challenges," *VLSI Design*, vol. 2012, pp. 716476-1-13, 2012.

[2] S. Haykin, "Cognitive radio: Brain-empowered wireless communications," *IEEE J. Sel. Areas Commun.*, vol. 23, no. 2, pp. 201–220, Feb. 2005.

[3] S. Roberts, "Radar & EW in the RAF," [Online]. Available: https://www.cambridgewireless.co.uk/media/uploads/resources

[4] J. Capmany, and D. Novak, "Microwave photonics combines two worlds," *Nat. Photon.*, vol. 1, no. 6, pp. 319–330, 2007.

[5] S. L. Pan and D. Zhu, "Broadband cognitive radio enabled by photonics," presented at the Proc. 45th European Conf. Exhibition Opt. Commun., Dublin, Ireland, Sep. 18–26, 2019.

[6] P. Ghelfi *et al.*, "A fully photonics-based coherent radar system," *Nature*, vol. 507, no. 7492, pp. 341–345, 2014.

[7] S. L. Pan *et al.*, "Satellite payloads pay off," *IEEE Microw. Mag.*, vol. 16, no.8, pp. 61–73, 2015.

[8] S. Z. Gurbuz, H. D. Griffiths, A. Charlish, M. Rangaswamy, M. S. Greco, and K. Bell, "An overview of cognitive radar: Past, present, and future," *IEEE Aerosp. Electron. Syst. Mag.*, vol. 34, pp. 6–18, 2019.

[9] S. Pan and J. Yao, "Photonics-based broadband microwave measurement," *J. Lightw. Technol.*, vol. 35, no.16, pp. 3498–3513, 2016.

[10] X. Zou, B. Lu, W. Pan, L. Yan, A. Stöhr, and J. Yao, "Photonics for microwave measurements," *Laser Photon. Rev.*, vol. 10, no. 5, pp. 711–734, 2016.

[11] S. T. Winnall, A.C. Lindsay, M. W. Austin, J. Canning, and A. Mitchell, "A microwave channelizer and spectroscope based on an integrated optical bragg-grating fabry–Perot and integrated hybrid fresnel lens system," *IEEE Trans. Microw. Theory Techn.*, vol. 54, no. 2, pp. 868–872, 2006.

[12] D. B. Hunter, L. G. Edvell, and M. A. Englund, "Wideband microwave photonic channelised receiver," in *Proc. IEEE Int. Top. Meet. Microw. Photon.*, Seoul, Korea, 2005, pp. 249–252.

[13] S. Song, X. Yi, and T. Huang, "Microwave photonic channelized receiver based on double column microring array," in *Proc. IEEE Opto-Electro. Commun. Conf.*, 2015.

[14] C.-S. Bres *et al.*, "Parametric photonic channelized RF receiver," *IEEE Photon. Technol. Lett.*, vol. 23, no. 6, pp. 344–346, 2011.

[15] B. Camille-Sophie, Z. Sanja, A. O. J. Wiberg, and R. J. O. E. Stojan, "Reconfigurable parametric channelized receiver for instantaneous spectral analysis," *Opt. Express*, vol. 19, no. 4, pp. 3531–3541, 2011.

[16] C. Bres and A. O. Wiberg, "Characterization of parametric RF channelized receiver through time domain monitoring," in *Proc. Conf. Opt. Fiber Commun.*, 2012.

[17] X. Zou, W. Li, W. Pan, L. Yan, and J. Yao, "Photonic-assisted microwave channelizer with improved channel characteristics based on spectrum-controlled stimulated brillouin scattering," *IEEE Trans. Microw. Theory Techn.*, vol. 61, no. 9, pp. 3470–3478, 2013.

[18] X. Xie, Y. Dai, Y. Ji, K. Xu, Y. Li, J. Wu, and J. Lin, "Channelization based on a 39-GHz optical frequency comb," *IEEE Photon. Technol. Lett.*, vol. 24, no. 8, pp. 661–663, 2012.

[19] X. Zou, W. Pan, B. Luo, and L. Yan, "Photonic approach for multiple-frequency-component measurement using spectrally sliced incoherent source," *Opt. Lett.*, vol. 35, no. 3, pp. 438–440, 2010.

[20] J. R. Adleman, S. Zlatanovic, J. M. Kvavle, B. M. L. Pascoguin, and E. W. Jacobs, "High finesse compound optical ring filter for parametric multicasting RF channelization," *in Proc. IEEE Int. Top. Meet. Microw. Photon.*, 2013, pp. 257–260.

[21] X. Xu, J. Wu, M. Tan, T. G. Nguyen, S. T. Chu, B. E. Little *et al.*, "Broadband photonic RF channelizer based on micro-combs," *in Terahertz, RF, Millimeter, and Submillimeter-Wave Technol. Appl. XII*, 2019, p. 1091722.

[22] J. Wang *et al.*, "Photonic-assisted seamless channelization based on integrated three-stage cascaded DIs," *in Proc. IEEE Int. Top. Meet. Microw. Photon.,* 2014, pp. 21–24.

[23] S. J. Strutz and K. J. Williams "An 8-18-GHz all-optical microwave downconverter with channelization," *IEEE Trans. Microw. Theory Techn.*, vol. 49, no. 10, pp. 1992–1995, 2001.

[24] W. Wang *et al.*, "Characterization of a coherent optical RF channelizer based on a diffraction grating," *IEEE Trans. Microw. Theory Techn.*, vol. 49, no. 10, pp. 1996–2001, 2001.

[25] G. Gao and L. Lei, "Photonics-based broadband RF spectrum measurement with sliced coherent detection and spectrum stitching technique," *IEEE Photon. J.*, vol. 9, no. 5, pp. 5503111-1-11, 2017.

[26] W. Y. Xu, D. Zhu, and S. L. Pan, "Coherent photonic radio frequency channelization based on dual coherent optical frequency combs and stimulated Brillouin scattering," *Opt. Eng.*, vol. 55, no. 4, pp. 046106, 2016.

[27] W. Y. Xu, D. Zhu, and S. L. Pan, "Coherent photonic RF channelization based on stimulated brillouin scattering," in *Proc. IEEE Int. Top. Meet. Microw. Photon.*, Paphos, Cyprus, 2015, pp. 15667908-1-4.

[28] X. Xu *et al.*, "Broadband RF channelizer based on an integrated optical frequency Kerr comb source," *J. Lightw. Technol.* vol. 36, no. 19, pp. 4519–4526, 2018.

[29] W. Hao *et al.*, "Chirped-pulse-based broadband RF channelization implemented by a mode-locked laser and dispersion," *Opt. Lett.*, vol. 42, no. 24, pp. 5234–5237, 2017.

[30] D. Zhu and S. L. Pan, "Photonics-based microwave image-reject mixer," *MDPI Photon.*, vol. 5, no. 2, pp. 6-1-12, 2018.

[31] X. Xie *et al.*, "Broadband photonic RF channelization based on coherent optical frequency combs and I/Q demodulators," *IEEE Photon. J.*, vol. 4, no. 4, pp. 1196–1202, 2012.

[32] A. O. J. Wiberg *et al.*, "Photonic RF-channelized receiver based on wideband parametric mixers and coherent detection," in *Proc.Conf. Lasers Electro-Optics IEEE-Laser Sci. Photon.* Appl., 2014, pp. 1–2.

[33] A. O. J. Wiberg *et al.*, "Coherent filterless wideband microwave/millimeter-wave channelizer based on broadband parametric mixers," *J. Lightw. Technol.*, vol. 32, no. 20, pp. 3609–3617, 2014.

[34] D. Zhu, W. J. Chen, Z. W. Chen, T. H. Du, Z. Z. Tang and S. L. Pan, "RF Front-end Based on Microwave Photonics," in *in Proc. 12th Conf. Lasers and Electro-Optics Pacific Rim, 22nd Optoelectron. Commun. Conf., and 5th Photon. Global Conf.*, Singapore, Jul. 31- Aug. 4, 2017, pp. 1–3.

[35] Z. Z. Tang, D. Zhu, and S. L. Pan, "Coherent optical RF channelizer with large instantaneous bandwidth and large in-band interference suppression," *J. Lightw. Technol.*, vol. 36, no. 19, pp. 4219–4226, 2018.

[36] W. J. Chen, D. Zhu, C. X. Xie, J. Liu, and S. L. Pan, "Microwave channelizer based on a photonic dual-output image-reject mixer," *Opt. Lett.*, vol. 44, no. 16, pp. 4052–4055, Aug. 2019.

[37] C. X. Xie, D. Zhu, W. J. Chen and S. L. Pan, "Microwave photonic channelizer based on polarization multiplexing and photonic dual output image reject mixer", *IEEE Access*, vol.7, pp. 158308–158316, Oct. 2019

[38] D. Zhu, W. J. Chen, and S. L. Pan, "Photonics-enabled balanced Hartley architecture for broadband image-reject microwave mixing," *Opt. Express*, vol. 26, no. 21, pp. 28022–28029, 2018.

[39] H. Chen *et al.*, "Photonics-assisted serial channelized radio-frequency measurement system with Nyquist-bandwidth detection," *IEEE Photon. J.*, vol. 6, no. 6, 2014, Art. no. 7903707.

[40] R. Li, H. Chen, Y. Yu, M. Chen, S. Yang, and S. Xie, "Multiple-frequency measurement based on serial photonic channelization using optical wavelength scanning," *Opt. Lett.*, vol. 38, no. 22, pp. 4781–4784, 2013.

[41] R. Li *et al.*, "Optical serial coherent analyzer of radio-frequency (OSCAR)," *Opt. Express*, vol. 22, no. 11, pp. 13579–13585, 2014.

[42] D. Onori *et al.*, "A photonically enabled compact 0.5–28.5 GHz RF scanning receiver," *J. Lightw. Technol.*, vol. 36, no. 10, pp. 1831–1839, 2018.

[43] T. A. Nguyen, E. H. Chan, and R. A. Minasian, "Photonic multiple frequency measurement using a frequency shifting recirculating delay line structure," *J. Lightw. Technol.*, vol. 32, no. 20, pp. 3831–3838, 2014.

[44] L. Cheng, M. Chen, H. Chen, S. Yang, and S. Xie, "Recirculating frequency shifting based photonic-assisted broadband instantaneous radio-frequency measurement," in *in CLEO: Sci. Innovations*, 2014, pp. SM1G–8.

[45] L. Cheng, H. Chen, R. Li, M. Chen, S. Yang, and S. Xie, "Broadband high-resolution programmable radio frequency signal analysis," *SPIE Newsroom*, DOI: 10.1117/2.1201411.005652, 2014.

[46] T. A. Nguyen, E. H. W. Chan, and R. A. Minasian, "Instantaneous high-resolution multiple-frequency measurement system based on frequency-to-time mapping technique," *Opt. Lett.*, vol. 39, no. 8, pp. 2419–2422, 2014.

[47] X. Wang *et al.*, "Wideband adaptive microwave frequency identification using an integrated silicon photonic scanning filter," *Photon. Res.*, vol. 7, no.2, pp. 172–181, 2019.

[48] X. Long, W. Zou, and J. Chen, "Broadband instantaneous frequency measurement based on stimulated Brillouin scattering," *Opt. Express*, vol. 25, no. 3, pp. 2206–2214, 2017.

[49] W. Zou, X. Long, X. Li, G. Xin, and J. Chen, "Brillouin instantaneous frequency measurement with an arbitrary response for potential real-time implementation," *Opt. Lett.*, vol. 44, no. 8, pp. 2045–2048, 2019.

[50] P. D. Welch, "The use of fast Fourier transform for the estimation of power spectra: A method based on time averaging over short, modified periodograms," *IEEE Trans. Audio Electroacoust.*, vol. 15, no. 2, pp. 70–73, 1967.

[51] R. Salem, M. A. Foster, and A. L. Gaeta, "Application of space-time duality to ultrahigh-speed optical signal processing," *Adv. Opt. Photon.*, vol. 5, pp. 274–317, 2013.

[52] T. Jannson, "Real-time Fourier transformation in dispersive optical fibers," *Opt. Lett.*, vol. 8, no. 4, pp. 232–234, 1983.

[53] M. A. Muriel, J. Azaña, and A. Carballar, "Real-time Fourier transformer based on fiber gratings," *Opt. Lett.*, vol. 24, no. 1, pp. 1–3, 1999.

[54] Y. Zheng, J. L. Li, Y. T. Dai, F. F. Yin and K. Xu, "Real-time Fourier transformation based on the bandwidth magnification of RF signals," *Opt. Lett.*, vol. 43, no. 2, pp. 194–197, 2018.

[55] R. E. Saperstein, D. Panasenko, and Y. Fainman, "Demonstration of a microwave spectrum analyzer based on time-domain optical processing in fiber," *Opt. Lett.*, vol. 29, no. 5, pp. 501–503, 2004.

[56] Y. H. Duan, L. Chen, H. D. Zhou, X. Zhou, C. Zhang, and X. L. Zhang, "Ultrafast electrical spectrum analyzer based on all-optical Fourier transform and temporal magnification," *Opt. Express*, vol. 25, no. 7, pp. 7520–7529, 2017.

[57] Y. H. Duan, L. Chen, L. Zhang, X. Zhou, C. Zhang, and X. L. Zhang, "Temporal radio-frequency spectrum analyzer, based on asynchronous optical sampling assisted temporal convolution," *Opt. Express*, vol. 26, no. 16, pp. 20735–20743, 2018.

[58] H. G. D. Chatellus, L. R. Cortés, and J. Azaña, "Optical real-time Fourier transformation with kilohertz resolutions," *Optica*, vol. 3, no. 1, pp. 1–8, 2016.

[59] W. Namgoong, "A channelized digital ultrawideband receiver," *IEEE Trans. Wireless Commun.*, vol. 2, pp. 502–510, 2003.

[60] J. Chou, Y. Han, and B. Jalali, "Adaptive RF-photonic arbitrary waveform generator," *IEEE Photon. Technol. Lett.*, vol. 15, no. 4, pp. 581–583, 2003.

[61] F. Zhang, X. Ge, and S. Pan, "Background-free pulsed microwave signal generation based on spectral shaping and frequency-to-time mapping," *Photon. Res.*, vol. 2, no. 4, pp. B5–B10, 2014.

[62] D. E. Leaird and A. M. Weiner, "Femtosecond direct space-to-time pulse shaping in an integrated-optic configuration," *Opt. Lett.*, vol. 29, no. 13, pp. 1551–1553, 2004.

[63] Y. Li, A. Rashidinejad, J.-M. Wun, D. E. Leaird, J.-W. Shi, and A. M. Weiner, "Photonic generation of W-band arbitrary waveforms with high time-bandwidth products enabling 3.9 mm range resolution," *Optica*, vol. 1, no. 6, pp. 446–454, 2014.

[64] J. Yao, "Microwave photonics: Arbitrary waveform generation," *Nat. Photon.*, vol. 4, no. 2, pp. 79–80, 2010.

[65] C. Wang and J. Yao, "Phase-coded millimeter-wave waveform generation using a spatially discrete chirped fiber Bragg Grating," *IEEE Photon. Technol. Lett.*, vol. 24, no. 17, pp. 1493–1495, 2012.

[66] M. Kahn *et al.*, "Ultrabroad-bandwidth arbitrary radiofrequency waveform generation with a silicon photonic chip-based spectral shaper," *Nat. Photon.*, vol. 4, no. 2, pp. 117–122, 2010.

[67] J. Zhang, O. L. Coutinho, and J. P. Yao, "Photonic generation of a linearly chirped microwave waveform with extended temporal duration using a dispersive loop," *IEEE Trans. Microw. Theory Techn.*, vol. 64, no. 6, pp. 1947–1953, 2016.

[68] Z. Jiang, C.-B. Huang, D. E. Leaird, and A. M. Weiner, "Optical arbitrary waveform processing of more than 100 spectral comb lines," *Nat. Photon.*, vol. 1, no. 8, pp. 463–467, 2007.

[69] S.-C. Chan, "Analysis of an Optically injected semiconductor laser for microwave generation," *IEEE J. Quantum Electron.*, vol. 46, pp. 421–428, 2010.

[70] S. K. Hwang, J. M. Liu, and J. K. White, "Characteristics of period-one oscillations in semiconductor lasers subject to optical injection," *IEEE J. Sel. Top. Quantum Electron.*, vol. 10, pp. 974–981, 2004.

[71] P. Perez *et al.*, "Photonic generation of microwave signals using a single-mode VCSEL subject to dual-beam orthogonal optical injection," *IEEE Photon. J.*, vol. 7, no. 1, pp. 5500614-1-14, 2015.

[72] C. Wang, R. Raghunathan, K. Schires, S. C. Chan, L. F. Lester, and F. Grillot, "Optically injected InAs/GaAs quantum dot laser for tunable photonic microwave generation," *Opt. Lett.*, vol. 41, pp. 1153–1156, 2016.

[73] F. Li *et al.*, "Subharmonic microwave modulation stabilization of tunable photonic microwave generated by period-one nonlinear dynamics of an optically injected semiconductor laser," *J. Lightw. Technol.*, vol. 32, no. 23, pp. 4660–4666, 2014.

[74] J. Zhuang and S. Chan, "Tunable photonic microwave generation using optically injected semiconductor laser dynamics with optical feedback stabilization," *Opt. Lett.*, vol. 38, pp. 344–346, 2013.

[75] J. P. Zhuang and S. C. Chan, "Phase noise characteristics of microwave signals generated by semiconductor laser dynamics," *Opt. Express*, vol. 23, no. 3, pp. 2777–2797, 2015.

[76] S. Pan and J. Yao, "Wideband and frequency-tunable microwave generation using an optoelectronic oscillator incorporating a Fabry-Perot laser diode with external optical injection," *Opt. Lett.*, vol. 35, pp. 1911–1913, 2010.

[77] P. Zhou, F. Zhang, B. Gao, and S. Pan, "Optical pulse generation by an optoelectronic oscillator with optically injected semiconductor laser," *IEEE Photon. Technol. Lett.*, vol. 28, no. 17, pp. 1827–1830, 2016.

[78] C. Xue, S. Ji, A. Wang, N. Jiang, K. Qiu, and Y. Hong, "Narrow-linewidth single-frequency photonic microwave generation in optically injected semiconductor lasers with filtered optical feedback," *Opt. Lett.*, vol. 43, no. 17, pp. 4184–4187, 2018.

[79] P. Zhou, F. Zhang, X. Ye, Q. Guo, and S. Pan, "Flexible frequency-hopping microwave generation by dynamic control of optically injected semiconductor laser," *IEEE Photon. J.*, vol. 8, no. 6, pp. 1–9, 2016.

[80] P. Zhou, F. Zhang, Q. Guo, S. Li, and S. Pan, "Reconfigurable radar waveform generation based on an optically injected semiconductor laser," *IEEE J. Sel. Topics Quantum Electron.*, vol. 23, no. 6, pp. 1801109- 1–9, 2017.

[81] P. Zhou, F. Zhang, Q. Guo, and S. Pan, "Linearly chirped microwave waveform generation with large time-bandwidth product by optically injected semiconductor laser," *Opt. Express*, vol. 24, no. 16, pp. 18460–18467, 2016.

[82] Y. Wang, J. Zhang, O. L. Coutinho, and J. P. Yao, "Interrogation of a linearly chirped fiber Bragg grating sensor with a high resolution using a linearly chirped optical waveform," *Opt. Lett.*, vol. 40. no. 21, pp. 4923–4926, 2015.

[83] B. W. Zhang, D. Zhu, P. Zhou, C. X. Xie, and S. L. Pan, "Tunable triangular frequency modulated microwave waveform generation with improved linearity using an optically injected semiconductor laser," *Appl. Opt.*, vol. 58, no. 20, pp. 5479–5485, 2019.

[84] J. P. Zhuang, X. Z. Li, S. S. Li, and S. C. Chan, "Frequency-modulated microwave generation with feedback stabilization using an optically injected semiconductor laser," *Opt. Lett.*, vol. 41, no. 24, pp. 5764–5767, 2016.

[85] T. A. Schaffer, H. P.Warren, M. J. Bustamante, K. W.Kong, "A 2 GHz 12-bit digital-to-analog converter for direct digital synthesis applications", *Techn. Digest GaAs Ie Symp.*, 1996, pp. 61–64.

[86] A. Yacoubian and P. K. Das, "Digital-to-analog conversion using electrooptic modulators," *IEEE Photon. Technol. Lett.*, vol. 15, no. 1, pp.117–119, 2003.

[87] M. Currie and J. W. Lou, "Weighted, summing photonic digital-to-analog converter," *Electron. Lett.*, vol. 42, no. 1, pp. 54–55, 2006.

[88] X. Yu, K. Wang, X. Zheng, and H. Zhang, "Incoherent photonic digital-to-analogue converter based on broadband optical source," *Electron. Lett.*, vol. 43, no. 19, pp. 1044–1045, 2007.

[89] A. Leven *et al.*, "High speed integrated InP photonic digital-to-analog converter," in *Proc. Indium Phosphide Related Materials Conf.,* 2006, pp. 14–15.

[90] A. Leven, J. Lin, J. Lee, K.-Y. Tu, Y. Baeyens, and Y. K. Chen, "A 12.5 Gsample/s optical digital-to-analog converter with 3.8 effective bits," in *Proc. 17th Annual Meet. IEEE Lasers and Electro-Optics Society ,* Puerto Rico, 2004, pp. 270–271.

[91] S. Oda and A. Maruta, "All-optical digital-to-analog conversion using nonlinear optical loop mirrors," *IEEE Photon. Technol. Lett.*, vol. 18, no. 5, pp. 703–705, 2006.

[92] F. Zhang, B. Gao, S. Pan, "Two-bit photonic digital-to-analog conversion unit based on polarization multiplexing," *Opt. Eng.*, vol. 55, no. 3, pp.031115-1-4, 2016.

[93] J. Ding *et al.*, "Optical digital-to-analog converter based on microring switches," *IEEE Photon. Technol. Lett.*, vol. 26, no. 20, pp. 2066–2069, 2014.

[94] J. Liao *et al.*, "Novel bipolar photonic digital-to-analog conversion employing differential phase shift keying modulation and balanced detection," *IEEE Photon. Technol. Lett.*, vol. 25, no. 2, pp. 126–128, 2013.

[95] T. Saida, K. Okamoto, K. Uchiyama, K. Takiguchi, T. Shibata, and A. Sugita, "Integrated optical digital-to-analogue converter and its application to pulse pattern recognition," *Electron. Lett.*, vol. 37, no. 20, pp.1237–1238, 2001.

[96] T. Nishitani, T. Konishi, H. Furukawa, and K. Itoh, "All-optical digital-to-analog conversion using pulse pattern recognition based on optical correlation processing," *Opt. Express*, vol. 13, no. 25, pp.10310–10315, 2005.
[97] Y. Peng *et al.*, "Photonic digital-to-analog converter based on summing of serial weighted multiwavelength pulses," *IEEE Photon. Technol. Lett.*, vol. 20, no. 24, pp. 2135–2137, 2008.
[98] B. Gao, F. Zhang, S. L. Pan, "Experimental demonstration of arbitrary waveform generation by a 4-bit photonic digital-to-analog converter," *Opt. Commun.*, vol. 383, pp.191–196, 2017.
[99] M. A. Richards, *Fundamentals of Radar Signal Processing*, Tata McGraw-Hill Education, 2014.
[100] H. Gao, C. Lei, M. Chen, F. Xing, H. Chen, and S. Xie, "A simple photonic generation of linearly chirped microwave pulse with large time-bandwidth product and high compression ratio," *Opt. Express*, vol. 21, pp. 23107–23115, 2013.
[101] J. W. Shi, F. M. Kuo, C. Nan-Wei, S. Y. Set, C. B. Huang, and J. E. Bowers, "Photonic Generation and wireless transmission of linearly/nonlinearly continuously tunable chirped millimeter-wave waveforms with high time-bandwidth product at w-band," *IEEE Photon. J.*, vol. 4, no. 1, pp. 215–223, 2012.
[102] J. M. Wun, C. C. Wei, J. Chen, C. S. Goh, S. Y. Set, and J. W. Shi, "Photonic chirped radio-frequency generator with ultra-fast sweeping rate and ultra-wide sweeping range," *Opt. Express*, vol. 21, no. 9, pp. 11475–81, 2013.
[103] O. L. Coutinho, J. Zhang, and J. P. Yao, "Photonic generation of a linearly chirped microwave waveform with a large time-bandwidth product based on self-heterodyne technique," *in Proc. IEEE Int. Top. Meet. Microw. Photon., Paphos*, Cyprus, 2015.
[104] X. Wang, J. Ma, Q. Zhang, and X. Xin, "Generation of linear frequency-modulated signals with improved time-bandwidth product based on an optical frequency comb," *Appl. Opt.*, vol. 58, no. 25, pp. 3222–3228, 2019.
[105] W. Chen, D. Zhu, C. Xie, T. Zhou, X. Zhong, and S. Pan, "Photonics-based reconfigurable multi-band linearly frequency-modulated signal generation," *Opt. Express*, vol. 26, no. 25, pp. 32491–32499, 2018.
[106] Q. Cen *et al.*, "Low phase noise linearly chirped microwave pulse based on opto-electronic oscillator," in *Proc. IEEE Int. Top. Meet. Microw. Photon.*, 2016, pp. 102–105.
[107] T. Hao *et al.*, "Breaking the limitation of mode building time in an optoelectronic oscillator," *Nat. Commun.*, vol. 9, pp. 1839-1-8, 2018.
[108] T. Hao, J. Tang, W. Li, N. Zhu, and M. Li, "Tunable fourier domain mode-locked optoelectronic oscillator using stimulated brillouin scattering," *IEEE Photon. Technol. Lett.*, vol. 30, no. 21, pp. 1842–1845, 2018.
[109] Y. K. Chembo, D. Brunner, M. Jacquot, and L. Larger, "Optoelectronic oscillators with time-delayed feedback," *Rev. Modern Phys.*, vol. 91, no. 3, p. 035006-1-51, 2019.
[110] X. S. Yao and L. Maleki, "Optoelectronic microwave oscillator," *J. Opt. Soc. of America B*, vol. 13, no. 8, pp. 1725–1735, 1996.
[111] A. Amar and Y. Buchris, "Asynchronous transmitter position and velocity estimation using a dual linear chirp," *IEEE Signal Process. Lett.*, vol. 21, no. 9, pp. 1078–1082, 2014.
[112] S. Kim, I. Paek, and M. Ka, "Simulation and test results of triangular fast ramp FMCW waveform," *in Proc. of IEEE Radar Conf.*, 2003, pp. 1–4.
[113] H. Cheng, X. Zou, B. Lu, and Y. Jiang, "High-resolution range and velocity measurement based on photonic LFM microwave signal generation and detection," *IEEE Photon. J.*, vol. 11, no. 1, pp. 1–8, 2019.
[114] D. Zhu and J. Yao, "Dual-chirp microwave waveform generation using a dual-parallel Mach-Zehnder modulator," *IEEE Photon. Technol. Lett.*, vol. 27, no. 13, pp. 1410–1413, 2015.
[115] X. Li, S. Zhao, Z. Zhu, K. Qu, T. Lin, and D. Hu, "Photonic generation of frequency and bandwidth multiplying dual-chirp microwave waveform," *IEEE Photon. J.*, vol. 9, no. 3, pp. 7104014-1-14, 2017.
[116] R. Kumar and S. K. Raghuwanshi, "A photonic scheme for the generation of dual linear chirp microwave waveform based on the external modulation technique and its airborne application," *Opt. Quantum Electron.*, vol. 49, no. 11, pp. 370-1-13, 2017.
[117] Y. Xu, T. Jin, H. Chi, S. Zheng, X. Jin, and X. Zhang, "Photonic generation of dual-chirp waveforms with improved time-bandwidth product," *IEEE Photon. Technol. Lett.*, vol. 29, no. 15, pp. 1253–1256, 2017.
[118] Q. Cen *et al.*, "Rapidly and continuously frequency-scanning opto-electronic oscillator," *Opt. Express*, vol. 25, no. 2, pp. 635–643, 2017.
[119] T. Hao, J. Tang, N. Shi, W. Li, N. Zhu, and M. Li, "Dual-chirp Fourier domain mode-locked optoelectronic oscillator," *Opt. Lett.*, vol. 44, no. 8, pp. 1912–1915, 2019.
[120] S. Zhu, M. Li, N. H. Zhu, and W. Li, "Transmission of dual-chirp microwave waveform over fiber with compensation of dispersion-induced power fading," *Opt. Lett.*, vol. 43, no. 11, pp. 2466–2469, 2018.
[121] S. Zhu, M. Li, N. H. Zhu, and W. Li, "Chromatic-dispersion-induced power-fading suppression technique for bandwidth-quadrupling dual-chirp microwave signals over fiber transmission," *Opt. Lett.*, vol. 44, no. 4, pp. 923–926, 2019.
[122] K. Zhang *et al.*, "Anti-chromatic dispersion transmission of frequency and bandwidth-doubling dual-chirp microwave waveform," *Opt. Lett.*, vol. 44, no. 16, pp. 4004–4007, 2019.
[123] R. J. Fitzgerald, "Effects of range-Doppler coupling on chirp radar tracking accuracy," *IEEE Trans. Aerosp. Electron. Syst.*, vol. *AES*-10, no.4, pp. 528–532, 1974.
[124] L. Bruno, P. Braca, J. Horstmann, and M. Vespe, "Experimental evaluation of the range-Doppler coupling on HF surface wave radars," *IEEE Geosci. Remote Sens. Lett.* vol. 10, no. 4, pp. 850–854, 2013.
[125] G. Li, H. D. Meng, X. G. Xia, and Y. N. Peng, "Range and velocity estimation of moving targets using multiple stepped-frequency pulse trains," *Sensors*, vol. 8, no. 2, pp. 1343–1350, 2008.
[126] Z. Lu *et al.*, "Broadband linearly chirped light source with narrow linewidth based on external modulation," *Opt. Lett.*, vol. 43, no. 17, pp. 4144–4147, 2018.
[127] M. Lu, M. Chang, Y. Deng, and P. Prucnal, "Performance comparison of optical interference cancellation system architectures," *Appl. Opt.*, vol. 52, no. 11, pp. 2484–2493, 2013.
[128] J. Suarez, K. Kravtsov, and P. R. Prucnal, "Incoherent method of optical interference cancellation for radio-frequency communications," *IEEE J. Quantum Electron.*, vol. 45, no. 4, pp. 402–408, 2009.
[129] X. Han, B. Huo, Y. Shao, C. Wang, and M. Zhao, "RF self-interference cancellation using phase modulation and optical sideband filtering," *IEEE Photon. Technol. Lett.*, vol. 29, no. 11, pp. 917–920, Jun. 2017.
[130] Y. Xiang, G. Li, and S. Pan, "Ultrawideband optical cancellation of RF interference with phase change," *Opt. Express*, vol. 25, no. 18, pp. 21259–21264, 2017.
[131] M. P. Chang, M. Fok, A. Hofmaier and P. R. Prucnal, "Optical analog self-Interference cancellation using electro-absorption modulators," *IEEE Microw. Wireless Compon. Lett.*, vol. 23, no. 2, pp. 99–101, 2013.
[132] Q. Zhou, H. Feng, G. Scott, and M. P. Fok, "Wideband co-site interference cancellation based on hybrid electrical and optical techniques," *Opt. Lett.*, vol. 39, no. 22, pp. 6537–6540, 2014.
[133] J. Chang and P. R. Prucnal, "A novel analog photonic method for broadband multipath interference cancellation," *IEEE Microw. Wireless Compon. Lett.*, vol. 23, no. 7, pp. 377–379, 2013.
[134] W. Zhou, P. Xiang, Z. Niu, M. Wang, S. Pan, "Wideband optical multipath interference cancellation based on a dispersive element," *IEEE Photon. Technol. Lett.*, vol. 28, no. 8, pp. 849–851, 2016.
[135] B. Weng, Y. Chen, and Y. Chen, "Photonic-assisted wideband frequency downconverter with self-interference cancellation and image rejection," *Appl. Opt.*, vol. 58, no.13, pp. 3539–3547, 2019.
[136] X. P. Hu, D. Zhu, W. J. Chen, D. Ben, and S. L. Pan, "Photonic simultaneous self-interference cancellation and image-reject mixing", in *Proc. Asia Comm. Photon. Conf.*, 2019, pp. M4C–8.
[137] D. Zhu, X. P. Hu, W. J. Chen, D. Ben, and S. L. Pan, "Photonics-enabled simultaneous self-interference cancellation and image-reject mixing", *Opt. Lett.*, vol. 44, no. 22, pp. 5541–5544, 2019.
[138] I. Brodsky, J. Brand, and M. Jain, "Freedom of frequency: How the quest for in-band full-duplex led to a breakthrough in filter design," *IEEE Microw. Mag.*, vol. 20, no. 2, pp. 36–43, 2019.
[139] R. M. Li *et al.*, "Synthetic aperture radar based on photonic-assisted signal generation and processing," in *2017 Opto-Electron. Commun. Conf. Photon. Global Conf.*, Singapore, July. 2017, pp. 1–3.
[140] R. Li *et al.*, "Demonstration of a microwave photonic synthetic aperture radar based on photonic-assisted signal generation and stretch processing," *Opt. Express*, vol. 25, no. 13, pp. 14334–14340, 2017.
[141] F. Zhang *et al.*, "Photonics-based broadband radar for high-resolution and real-time inverse synthetic aperture imaging," *Opt. Express*, vol. 25, no. 14, pp. 16274–16281, 2017.
[142] S. Pan and F. Zhang, "Ultra-high resolution real-time radar imaging based on microwave photonics," in *Proc. 23rd Opto-Electron. Commun. Conf.,* Jeju *Island*, *Korea (South)*, 2018.
[143] A. Wang *et al.*, "Ka-band microwave photonic ultra-wideband imaging radar for capturing quantitative target information," *Opt. Express*, vol. 26, no. 16, pp. 20708–20717, 2018.

[144] X. W. Ye *et al.*, "Photonics-based radar with balanced I/Q dechirping for interference-suppressed high-resolution detection and imaging," *Photon. Res.*, vol. 7, no. 3, pp. 265–272, 2019.
[145] J. M. Cao *et al.*, "Photonic deramp receiver for dual-band LFM-CW radar," *J. Lightw. Technol.*, vol. 37, no. 10, pp. 2403-24-8, 2019.
[146] J. X. Zhang *et al.*, "Photonics-based simultaneous measurement of distance and velocity using multi-band LFM microwave signals with opposite chirps," *Opt. Express*, vol. 27, no. 20, pp. 27580–27591, 2019.
[147] Z. Y. Meng *et al.*, "Dual-band dechirping LFMCW radar receiver with high image rejection using microwave photonic I/Q mixer," *Opt. Express*, vol. 25, no. 18, pp. 22055–22065, 2017.
[148] P. Ghelfi, F. Laghezza, F. Scotti, D. Onori, and A. Bogoni, "Photonics for radars operating on multiple coherent bands," *J. Lightw. Technol.*, vol. 34, no. 2, pp. 500–507, 2016.
[149] F. Laghezza, F. Scotti, D. Onori and A. Bogoni, "ISAR imaging of non-cooperative targets via dual band photonics-based radar system,"in *Proc. 17th Int. Radar Symp.*, *Krakow*, Poland, 2016.
[150] F. Scotti, A. Bogoni, F. Laghezza, and D. Onori, "Tracking of a naval target with a dual-band photonic-based coherent radar system," in *IEEE Radar Conf.*, Philadelphia, PA, USA, 2016.
[151] S. Melo *et al.*, "Dual-use system combining simultaneous active radar & communication, based on a single photonics-assisted transceiver," in *Proc. 17th Int. Radar Symp., Krakow*, Poland, 2016.
[152] J. Shi, F. Zhang, X. Ye, Y. Yang, D. Ben, and S. Pan, "Photonics-based dual-functional system for simultaneous high-resolution radar imaging and fast frequency measurement," *Opt. Lett.*, vol. 44, no. 8, pp. 1948–1951, 2019.
[153] Fandiño J S *et al.*, "A monolithic integrated photonic microwave filter," *Nat. Photon.*, vol. 11, pp. 124–129, 2017.
[154] D. Marpaung *et al.*, "Low-power, chip-based stimulated Brillouin scattering microwave photonic filter with ultrahigh selectivity," *Optica*, vol. 2, no.2, pp. 76–83, 2015.
[155] Z. Z. Tang, Y. F. Li, J. P. Yao, and S. L. Pan, "Photonics-based microwave frequency mixing: methodology and applications," *Laser Photon. Rev.*, vol. 14, no. 1, pp. 1800350-1-25, Jan. 2020.
[156] X. Zou *et al.*, "A multifunctional photonic integrated circuit for diverse microwave signal generation, transmission, and processing," *Laser Photon. Rev.*, vol. 13, no. 6, pp. 1800240-1-10, 2019.

Dan Zhu (Member, IEEE) received the B.S. and Ph.D. degrees in electronic engineering from Tsinghua University, Beijing, China, in 2004 and 2009, respectively. In July 2009, she joined the Research Department of Signal Processing, No. 14 Research Institute, China Electronics Technology Group Corporation, as a Researcher. In May 2011, she joined the Key Laboratory of Radar Imaging and Microwave Photonics, Ministry of Education, Nanjing University of Aeronautics and Astronautics, Nanjing, China, where she is now an associate professor. Her current research interests include microwave photonic signal processing and the system applications. Dr. Zhu is a member of the IEEE Microwave Theory and Techniques Society, the IEEE Photonics Society, and the Optical Society of America.

Shilong Pan (Senior Member, IEEE) received the B.S. and Ph.D. degrees in electronic engineering from Tsinghua University, Beijing, China, in 2004 and 2008, respectively. From 2008 to 2010, he was a "Vision 2010" Postdoctoral Research Fellow in the Microwave Photonics Research Laboratory, University of Ottawa, Canada. He joined the College of Electronic and Information Engineering, Nanjing University of Aeronautics and Astronautics, China, in 2010, where he is currently a Full Professor and an Executive Director of the Key Laboratory of Radar Imaging and Microwave Photonics, the Ministry of Education. His research has focused on microwave photonics, which includes optical generation and processing of microwave signals, analog photonic links, photonic microwave measurement, and integrated microwave photonics. Prof. Pan has authored or co-authored over 420 research papers, including more than 240 papers in peer-reviewed journals and 190 papers in conference proceedings. Prof. Pan is currently an Associate Editor of *Electronics Letters*, a Topical Editor of *Chinese Optics Letters*, and is a Technical Committee Member of IEEE MTT-3 Microwave Photonics. He has also served as a Chair of a number of international conferences, symposia, and workshops, including the TPC Chair of the International Conference on Optical Communications and Networks in 2015, and TPC Co-chair of IEEE International Topical Meeting on Microwave Photonics in 2017. Prof. Pan is a Fellow of OSA, SPIE and IET, and a Senior Member of IEEE. He was selected as an IEEE Photonics Society Distinguished Lecturer in 2019.